Role of the Ectodomain of the gp41 Transmembrane Envelope Protein of Human Immunodeficiency Virus Type 1 in Late Steps of the Membrane Fusion Process

Séverine Bär and Marc Alizon*

Department of Cell Biology, Institut Cochin, INSERM U567, CNRS UMR8104, 75014 Paris, France

The membrane fusion process mediated by the gp41 transmembrane envelope glycoprotein of the human immunodeficiency virus type 1 (HIV-1) was addressed by a flow cytometry assay detecting exchanges of fluorescent membrane probes (DiI and DiO) between cells expressing the HIV-1 envelope proteins (Env) and target cells. Double-fluorescent cells were detected when target cells expressed the type of chemokine receptor, CXCR4 or CCR5, matching the type of gp120 surface envelope protein, X4 or R5, respectively. Background levels of double-fluorescent cells were observed when the gp120-receptor interaction was blocked by AMD3100, a CXCR4 antagonist. The L568A mutation in the N-terminal heptad repeat (HR1) of gp41 resulted in parallel inhibition of the formation of syncytia and double-fluorescent cells, indicating that gp41 had a direct role in the exchange of fluorescent probes. In contrast, three mutations in the loop region of the gp41 ectodomain, located on either side of the Cys-$(X)_5$-Cys motif (W596 M and W610A) or at the distal end of HR1 (D589L), had limited or no apparent effect on membrane lipid mixing between Env$^+$ and target cells, while they blocked formation of syncytia and markedly reduced the exchanges of cytoplasmic fluorescent probes. The loop region could therefore have a direct or indirect role in events occurring after the merging of membranes, such as the formation or dilation of fusion pores. Two types of inhibitors of HIV-1 entry, the gp41-derived peptide T20 and the betulinic acid derivative RPR103611, had limited effects on membrane exchanges at concentrations blocking or markedly reducing syncytium formation. This finding confirmed that T20 can inhibit the late steps of membrane fusion (post-lipid mixing) and brought forth an indirect argument for the role of the gp41 loop region in these steps, as mutations conferring resistance to RPR103611V were mapped in this region (I595S or L602H).

Human immunodeficiency virus type 1 (HIV-1) and other retroviruses deliver their replicative material into target cells after fusion of their lipidic envelope with the plasma membrane. This task is performed by a class of viral glycoproteins that are anchored within the envelope by a membrane-spanning domain and that are thus designated transmembrane envelope proteins (TM)—gp41 in the case of HIV-1. In virions or at the surface of infected cells, TM proteins are associated and largely masked by another class of envelope proteins termed surface (SU; gp120 for HIV-1) proteins, which are derived from the same precursor encoded by the viral *env* gene (43, 54). Access of the TM to the target cell membrane therefore requires partial or complete disruption of the SU/TM complex, which occurs after the interaction of SU with its cell surface receptor(s) (37). In the case of HIV-1, the membrane fusion process is initiated by the interaction of gp120 with a G protein-coupled receptor, either the CCR5 or the CXCR4 chemokine receptor, generally after prior contact of gp120 with another type of cell surface protein, CD4 (reviewed in references 2, 4, and 17). Viral envelope proteins such as the influenza virus hemagglutinin (HA2) are activated upon exposure to acidic pH and therefore mediate fusion with the membranes of endosomes (47), but the TMs of HIV-1 and most other

retroviruses are active at neutral pH and can mediate fusion with the plasma membrane (48). This ability also allows cells expressing HIV-1 envelope proteins (gp120 or gp41) to fuse and form syncytia with target cells that express the appropriate receptors.

There is no consensus on the exact mechanism by which retroviral TMs (or other viral proteins) accomplish membrane fusion. The present view is that they first engage contact with the target cell membrane by their amino-terminal hydrophobic domains, termed fusion peptides, and then undergo conformation changes in order to bring the viral and cellular lipid bilayers in proximity, allowing their external leaflets to merge, thereby forming a hemifusion intermediate. Next, an aqueous connection, termed a fusion pore, must open across the internal leaflets of the merged membranes and expand to leave open passage to the nucleocapsid (reviewed in references 3, 14, and 24). Retroviral TMs consist of an amino-terminal extracellular domain (or ectodomain), a membrane-spanning domain, and a carboxy-terminal cytoplasmic (or intraviral) domain. Mutations in the cytoplasmic domain can modify the efficiency of membrane fusion, either in a positive or a negative way, but the TM can continue to function despite the cytoplasmic domain's complete deletion, at least in syncytium-formation assays (18, 20). Fusion activity is also observed when the gp41 ectodomain is anchored by the membrane-spanning domain of an unrelated protein such as CD4 (53). Therefore, only the ectodomain of retroviral TMs seems to have a direct role in the membrane fusion process.

---

* Corresponding author. Mailing address: Institut Cochin, 22 rue Méchain, 75014 Paris, France. Phone: 33-1-40-51-64-86. Fax: 33-1-40-51-64-54. E-mail: alizon@cochin.inserm.fr.

Like other viral fusogenic proteins, such as the influenza virus HA2 (47), the Ebola virus GP2 (50), or the paramyxovirus F protein (1), retroviral ectodomains are characterized by the presence of two α-helix regions with propensity to form coiled coils that are termed heptad repeats (reviewed in reference 14). In the case of HIV-1 gp41, synthetic peptides corresponding to the amino-terminal (HR1) and carboxy-terminal (HR2) heptad repeats associate in solution to yield a tight protease-resistant 3:3 complex (32). X-ray crystallography revealed a six-helix bundle structure with a central coiled coil formed by three parallel HR1s against which three HR2s are packed in antiparallel orientation (9, 49, 51). A similar structure was observed by nuclear magnetic resonance or X-ray crystallography in the ectodomain of other retroviral TMs, the simian immunodeficiency virus (SIV) gp41 (7, 34), the human T-lymphotropic virus type 1 gp21 (27), and the Moloney murine leukemia virus p15E (19). In all retroviruses, the two helices are separated by a region of variable length containing a highly characteristic Cys-$(X)_{5-7}$-Cys motif, in which the two Cys residues are engaged in a disulfide link (21). This loop region also allows reversal of the chain orientation necessary for the packing of the HR2 helices on the central coiled coil. The two helices and the intervening loop region can therefore be envisioned as forming a hairpin, with the amino-terminal fusion peptide pointing toward the viral membrane and the disulfide-bonded Cys motif oriented toward the SU—a finding which is in agreement with the role of several residues of the loop region in the stability of the SU/TM complex (23, 33). But the loop region of gp41 must be accessible at some stage, since it corresponds to an immunodominant B epitope in the case of HIV-1 and other lentiviruses (12, 22).

According to the model initially proposed by Weissenhorn et al. (51), the hairpin structure may represent the stable and final conformation adopted by the ectodomain of gp41 or other retroviral TMs during the fusion process (10). This model envisions the existence of another gp41 conformation, termed the prehairpin, in which the HR1 and HR2 helices are not packed together but rather are dissociated so that the fusion peptide is projected toward the target cell membrane. Transition from this metastable conformation to the stable hairpin structure would provide the force needed to drive the merging of the two membranes. This model and the existence of the prehairpin structure are supported by three lines of arguments: (i) structural analogies between retroviral TMs and the influenza virus HA2, for which transition from inactive to fusion-active conformation could be analyzed by X-ray crystallography (5); (ii) unmasking of epitopes in the core of the gp41 ectodomain after contact of gp120 with receptors (25); and (iii) a transdominant-negative effect on gp41-mediated fusion and HIV-1 entry of peptides corresponding to the C-terminal helix (HR2) of HIV-1 gp41, in particular T20 (also known as DP178) (52). However, objections can be raised to these different arguments and to the hypothesis of a prehairpin structure (7, 26), which led to the proposal of other models for gp41-mediated membrane fusion (reviewed in reference 14).

Available models of membrane fusion offer very limited information on the role of the retroviral TMs (or other viral fusogenic proteins) in the events occurring posterior to the merging of lipid bilayers, schematically viewed as the formation of a fusion pore and its expansion. Most structure-function studies on retroviral TMs have indeed relied upon infection or syncytium formation assays, which cannot discriminate membrane lipid exchanges from subsequent events. This discrimination can be achieved by using assays based on the transfer of fluorescent membrane-associated probes, which have been extensively used for studies of different types of viral fusogenic proteins (reviewed in reference 3). In the case of HIV-1, this type of assay has been used to address the effects of antiviral peptides such as T20 (26, 38). It also allowed the researchers to show that the Trp-rich membrane-proximal domain of HIV-1 gp41 had a role in the late steps of the membrane fusion process (39). The assays used in these studies have a fluorescence microscopy readout and require relatively complex image acquisition and analysis techniques in order to yield quantitative results. To address the effect of mutations in gp41 on the exchanges of membrane lipids between cells expressing HIV-1 envelope proteins and target cells, we used a simpler quantitative assay based on flow cytometry. It detects the formation of double-fluorescent cells in cocultures of Env[+] and target cells labeled with distinct green or red lipophilic fluorescent probes. We found that two inhibitors of HIV-1 entry, the gp41-derived T20 peptide (52) and the betulinic acid derivative RPR10361 (36), had limited effects on membrane exchanges at concentrations blocking or markedly reducing syncytium formation. Several mutations in the immunodominant loop region of gp41 had a similar effect. These results confirm the role of the gp41 ectodomain in the late steps of the membrane fusion process.

MATERIALS AND METHODS

Cell lines. The HeLa-Env/LAI (46) and HeLa-Env/ADA cells (41) stably express gp120 or gp41 from the X4 HIV-1 strain LAI or the R5 HIV-1 strain ADA, respectively. Like HeLa-Δ*env* cells (46), they also express the HIV-1 transactivator Tat. The HeLa-P4 (13) and U373MG-CCR5 (28) target cell lines used in cell-cell fusion assays were both CD4^{+} and transfected with the *Escherichia coli* β-galactosidase gene (*lacZ*) under transcriptional control of the HIV-1 long terminal repeat. All cell lines used in this study were propagated in Dulbecco's modified Eagle's medium supplemented with 10% fetal calf serum, antibiotics (penicillin and streptomycin), and 2 mM glutamine.

Antibodies and chemical reagents. Goat anti-gp120 antibody and fluorescein isothiocyanate (FITC)-conjugated mouse anti-goat immunoglobulin G were purchased from Santa Cruz Biotechnology (Santa Cruz, Calif.). The fluorescent probes DiO (DiOC$_{18}$ [3], 3,3′-dioctadecyloxacarbocyanine perchlorate), DiI (DiIC$_{18}$ [3], 1,1′-dioctadecyl-3,3,3′,3′-tetramethylindocarbocyanine perchlorate), Cell Tracker Green (CTG; 5-chloromethyl-fluorescein-diacetate), and CMTMR (5-[and 6-]-[{(4-chloromethyl)benzoyl}amino]-tetramethylrhodamine) were purchased from Molecular Probes (Eugene, Oreg.). The AMD3100 bicyclam was obtained from G. Henson (AnorMED, Langley, British Columbia, Canada), betulinic acid derivative RPR103611 came from Y. Hénin (Aventis Laboratories, Vitry-sur-Seine, France), and T20 was from B. Labrosse (INSERM U552, Paris, France).

Expression of wild-type and mutant Env. Site-directed mutagenesis of gp41 was performed in the context of a previously described Env expression vector consisting of an HIV-1 LAI provirus with deletion of *gag* and *pol* genes and replacement of the viral *nef* gene by a methotrexate resistance gene (*dhfr*) (46). Cell lines stably expressing the D589L or W596 M mutant Env were obtained by transfection of HeLa cells and selection of methotrexate-resistant clones, as described previously (46). For transient expression studies, adherent HEK293T cells were transfected with wild-type (WT) or mutant Env vectors in six-well plates by a standard calcium phosphate technique. Expression of gp120 at the cell surface was monitored by flow cytometry 36 h after transfection. For this procedure, cells were detached in phosphate-buffered saline (PBS) with 1 mM EDTA, stained 1 h at 4°C with a goat anti-gp120 primary antibody (10 μg/ml in PBS with 2% fetal calf serum), treated for 45 min at 4°C with FITC-conjugated secondary antibody, and then fixed with 4% formaldehyde in PBS and analyzed on an Epics XL flow cytometer (Coultronics).

Syncytium formation assays. Approximately 2×10^5 target cells (HeLa-P4 or 373MG-CCR5) detached with PBS–1 mM EDTA were added to an equivalent number of adherent Tat$^+$ Env$^+$ cells (HeLa-Env/LAI, HeLa-Env/ADA, or transfected HEK293T cells) in a 35-mm plate (six wells). After 24 h, adherent cells were fixed with 0.5% glutaraldehyde in PBS and stained with the β-galactosidase substrate X-Gal (5-bromo-4-chloro-3-indolyl-β-D-galactopyranoside). Blue-stained foci representing syncytia were scored under ×20 magnification.

Membrane labeling and detection of fluorescent probe exchanges. The Env$^+$ and target cells were labeled with DiO (green fluorescence at 501 nm) and DiI (red fluorescence at 565 nm), respectively. To this end, adherent cells in six-well plates (~2×10^5 cells per well) were left in contact with DiI or DiO (2 μM in Dulbecco's modified Eagle's medium; 1 ml per well) for 2 min at room temperature. Labeling was ended by washing twice with PBS. Target cells were then detached with PBS–1 mM EDTA and added to an equivalent number of adherent Env$^+$ cells. In most experiments, membrane fluorescence was analyzed after a 2-h coculture at 37°C in cell culture medium. In certain experiments, cell-cell contact was initiated at 4°C for 2 h and fluorescence was analyzed at various times after shifting cells to a fusion-permissive temperature (37°C). Adherent cells were then washed with PBS, detached with trypsin, and fixed with 4% formaldehyde in PBS. Two-color fluorescence analysis was performed on an Epics XL flow cytometer with a 488-nm wavelength laser. Only cells displaying a relatively high level of fluorescence in the green and red wavelengths (>4 and >70 arbitrary log units, respectively) were scored as double-fluorescent cells. For confocal microscopy, the same protocol was used for labeling cells with DiI and DiO and coculture, except that Env$^+$ cells (stably transfected HeLa cells) were grown on glass coverslips in six-well plates in order to avoid detaching cells before they were fixed. Cocultures were observed on a Leica DMIRE2 microscope under ×63 magnification, ×2.5 zoom. Images were pseudocolored according to their respective emission wavelengths and overlaid with Metamorph software (Universal Imaging Corporation, West Chester, Pa.).

Detection of cytoplasmic exchanges. HEK293T cells were plated in six-well trays (~2×10^5 cells per well), transfected with WT or mutant HIV-1 Env expression vectors (6 μg/well), and either cotransfected with a green fluorescent protein (GFP) expression vector (pEGFP, 1.5 μg/well; Clontech) or labeled by a 45-min contact at 37°C with fluorescent probe CTG (10 μM) followed by 30 min in culture medium. The next day, adherent HeLa-P4 target cells were labeled by a 30-min contact with the red fluorescent probe CMTMR (8 μM in PBS) at 37°C and then washed with PBS, detached with PBS–1 mM EDTA, and resuspended in culture medium. CMTMR-labeled HeLa-P4 cells were added to adherent HEK293T cells, and cocultures were left for 2 h at 37°C. Adherent cells were detached with trypsin, fixed with 4% formaldehyde in PBS, and analyzed for red and green fluorescence on an Epics XL flow cytometer (experiments with GFP-labeled cells) or were fixed in situ and observed under fluorescence microscopy (CTG-labeled cells). In flow cytometry assays, cells were considered double fluorescent if their emissions were >3 log units in the red and green wavelengths. Otherwise, double-fluorescent cells were counted in random microscopical fields (×40 magnification).

RESULTS

Detection of membrane exchanges between cells expressing HIV-1 envelope proteins and target cells. Flow cytometry was used to detect and quantify exchanges of lipidic material between the plasma membranes of cells expressing the HIV-1 envelope proteins (Env$^+$ cells) and target cells during their fusion process. To this end, the two cell types were labeled with distinct membrane-associated fluorescent probes emitting in the red (DiI) or the green (DiO) wavelength. Membrane exchanges between Env$^+$ and target cells were expected to yield objects emitting fluorescence in the two wavelengths (double-fluorescent cells). The initial series of experiments was performed with a cell line stably expressing the Env proteins of a CXCR4-dependent (X4) HIV-1 strain (HeLa-Env/LAI) and a target cell line (HeLa-P4) expressing the CD4 and CXCR4 receptors. Target cells also harbor a reporter gene (long terminal repeat *lacZ*), allowing detection of syncytia formed with Tat$^+$ cells by staining with the β-galactosidase substrate X-Gal. The labeling conditions were chosen in order to obtain >98%

fluorescent cells (Fig. 1A and B) after a short time of contact (2 min) with a relatively low concentration of DiI or DiO (2 μM), which was expected to limit the amount of uptaken probe and therefore the possibility of its passive transfer, independent of membrane fusion. The labeling of Env$^+$ and target cells had no apparent effect on the cell-cell fusion process, as indicated by the similar numbers of syncytia detected in overnight cocultures of fluorescent or untreated cells (data not shown). After a 2-h contact of DiI-labeled HeLa-P4 and DiO-labeled HeLa-Env/LAI cells in a 1/1 ratio, two-color flow-cytometric analysis detected a population of cells with double fluorescence (Fig. 1C). Since a fraction of the DiO-labeled Env$^+$ cells have a detectable level of fluorescence in the DiI wavelength (Fig. 1B, quadrant 2b), we only took into consideration cells with the highest red fluorescence (>70 log units), corresponding to quadrant 2a in Fig. 1C. They represented ~8% of total cells analyzed ($n = 5,000$), but this fraction probably underestimates the number of double-fluorescent cells. There was indeed a marked increase of mean fluorescence intensity in the red wavelength (DiI) for the DiO-labeled Env$^+$ cells, from ~5 to 17 log units (Fig. 1D).

Since the formation of double-fluorescent cells could result from passive transfer of the fluorescent probes between cells, either totally independent of the HIV-1 envelope proteins or only dependent upon their ability to bind target cells, similar experiments were performed with Env-negative HeLa cells or with HeLa-Env/ADA cells stably expressing a CCR5-dependent (R5) Env, both of which are unable to form syncytia with HeLa-P4 target cells (Fig. 2A). Double-fluorescent cells could be detected in these cocultures, but in both cases they represented less than 1% of total cells analyzed (Fig. 2B), and there was no mean fluorescence intensity increase at the DiI wavelength (Fig. 1D). The background level of double-fluorescent cells therefore appeared to be independent of the expression of HIV-1 envelope proteins, which indicates that their interaction with CD4 or other surface elements of target cells, such as lectins, was not sufficient to trigger exchanges of the membrane dyes. The same conclusion could be reached from similar experiments performed with CCR5$^+$ U373MG target cells (CXCR4 negative). In that case, the formation of double-fluorescent cells was more efficient in cocultures with HeLa-Env/ADA cells than in those with HeLa-Env/LAI or Env-negative HeLa cells (Fig. 2B), both of which are unable to form syncytia with these target cells (Fig. 2A). The Env-independent background was more important than with X4 target cells, probably because of differences in the adhesion properties of HeLa and U373MG cells. Efficient formation of double-fluorescent cells occurred only if cells expressing one type of HIV-1 envelope protein (X4 or R5) were matched with target cells expressing the corresponding chemokine receptor, CXCR4 or CCR5, which is also the situation allowing membrane fusion and formation of syncytia.

Effect of inhibitors of HIV-1 entry. The role of membrane exchanges in the formation of double-fluorescent cells was further addressed by performing cocultures in the presence of different inhibitors of HIV-1 entry and Env-mediated cell-cell fusion, the AMD3100 bicyclam (15), a CXCR4 antagonist preventing its interaction with gp120 (28), the gp41-derived peptide T20 corresponding to the HR2 helix (52), and the betulinic acid derivative RPR103611 (36), which also targets gp41, al-
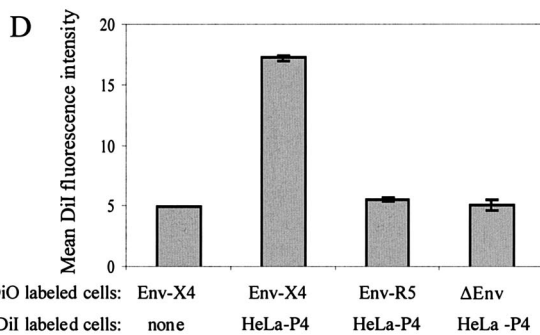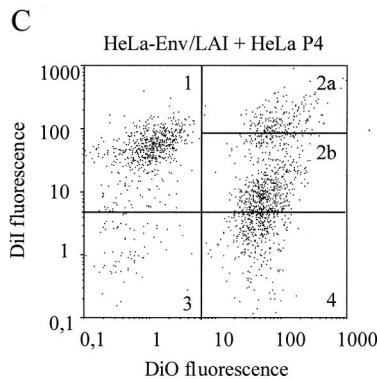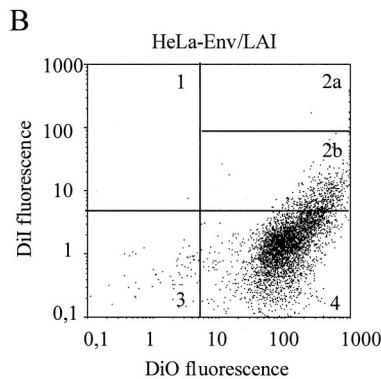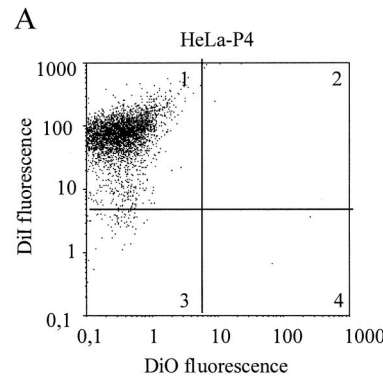
FIG. 1. Detection of membrane exchanges mediated by the HIV-1 envelope proteins (Env) between cells labeled with the fluorescent lipophilic probe DiI (red) or DiO (green). (A to C) Two-color flow cytometry analysis of HeLa-P4 cells (CD4$^+$ and CXCR4$^+$) labeled with DiI (A), of HeLa-Env/LAI cells labeled with DiO (B), and of a 2-h coculture of these two cell types (C) was initiated by adding HeLa-P4 cells to an equivalent number of adherent HeLa-Env/LAI cells. In each panel, ~5,000 fluorescent cells were analyzed. Quadrants 1 to 4 were defined for DiI-labeled cells so that >98% were
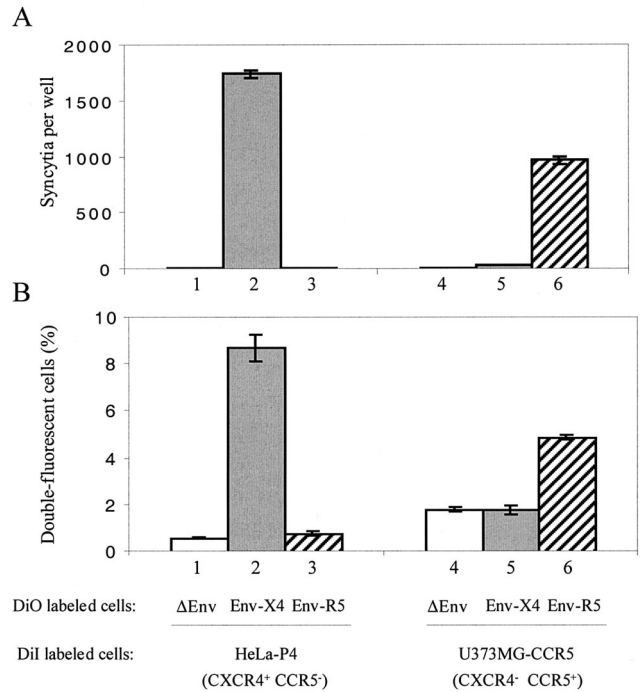

FIG. 2. Chemokine receptor and gp120 requirements for membrane exchanges and syncytium formation. Quantification of syncytia formed after overnight coculture (A) and of double-fluorescent cells formed after 2-h coculture of HeLa-P4 cells or U373-CCR5 target cells with an equivalent number of Env-negative HeLa cells (lanes 1 and 4), X4 Env$^+$ cells (HeLa-Env/LAI, lanes 2 and 5) or R5 Env$^+$ cells (HeLa-Env/ADA, lanes 3 and 6) (B). Cocultures were initiated by adding ~2 × 10^5 target cells to an equivalent number of adherent cells. Target cells were stably transfected with a Tat-inducible lacZ transgene, and their coculture partners expressed HIV-1 Tat, which allowed us to detect syncytia as blue foci after staining with X-Gal. In panel B, target cells were labeled with DiI, and coculture partners were labeled with DiO. Approximately 5,000 cells were analyzed by flow cytometry, and the percentage of double-fluorescent cells was determined as described in the legend of Fig. 1. Results represent the mean values from three independent experiments ± standard errors of the means.

though it is only active on certain X4 HIV-1 strains (29, 30). Cocultures of DiI-labeled HeLa-P4 and DiO-labeled HeLa-Env/LAI cells were initiated at 4°C (2 h) in order to allow cellular contacts but not membrane fusion; the cells were then shifted to 37°C in the presence or absence of the different inhibitors. Cocultures were analyzed by flow cytometry 3 h later or maintained overnight to quantify the formation of syncytia.

included in quadrant 1 (A). Since a fraction of the DiO-labeled cells had a detectable level of red fluorescence (quadrant 2 in panel B), only cells with the higher red fluorescence corresponding to subquadrant 2a in panel C were scored as double fluorescent. (D) Mean fluorescence intensity (MFI) at the DiI wavelength for DiO-labeled HeLa-Env/LAI cells (lane 1) and for cocultures of DiI-labeled HeLa-P4 cells with DiO-labeled HeLa-Env/LAI (lane 2), HeLa-Env/ADA (lane 3), or Env-negative HeLa cells (lane 4). Cocultures were performed and analyzed as described for panel C. The MFI at the DiI wavelength was calculated for the DiO-positive cells (corresponding to quadrants 2 and 4). Bars are the mean values from three independent experiments.

The three AMD3100 concentrations tested resulted in ~100% inhibition of the formation of syncytia (Fig. 3A) and markedly reduced formation of double-fluorescent cells (>80% inhibition), a finding which represents further evidence that this process requires the interaction of Env with the CXCR4 receptor. In contrast, RPR103611 and T20 seemed to have markedly lesser effects on the exchange of fluorescent probes than on the formation of syncytia. The lower concentration of RPR103611 tested (2.5 μM) resulted in ~100% inhibition of syncytia but only ~30% inhibition of the formation of double-fluorescent cells (Fig. 3B). The same discrepancy was observed for the T20 V peptide at the lower concentration tested (1 nM) since the formation of syncytia and double-fluorescent cells was reduced by ~75 and ~20%, respectively (Fig. 3C). Increasing the T20 V concentration to 40 nM and 4 μM further reduced the level of fluorescent probe exchange but did not block it. The RPR103611 and T20 compounds were therefore not devoid of activity on membrane exchanges, particularly at the higher concentrations tested, but they seem to interfere more efficiently with the formation of syncytia. An important part of their inhibitory activity may therefore be exerted after the lipid bilayers have merged.

Effect of mutations in the ectodomain of HIV-1 gp41. We next addressed the effect of single amino acid substitutions in the HIV-1 gp41 ectodomain on the efficiency of membrane exchanges with target cells. Mutations were selected because of their known inhibitory effects on syncytium formation (8). The modified residues, all conserved in the SIV ectodomain, were Leu568 (L568A) and Asp589 (D589L) in the N-terminal helix (HR1) and Trp596 (W596M) and Trp610 (W610A) in the loop region (Fig. 4). The mutant or WT Env was expressed in HEK293T cells by transient transfection. Flow cytometric analysis of transfected cells after staining with a polyclonal anti-gp120 antibody revealed similar levels of cell surface expression (~30% of cells were gp120 positive) for the WT and mutant Env (Fig. 5A). As expected, the mutations in gp41 markedly reduced (L568A) or almost abolished (D589L, W596M, and W610A) the formation of syncytia between transfected HEK293T cells and target HeLa-P4 cells (Fig. 5B). Unexpectedly, transfection of the W596M vector was found to activate expression of an endogenous β-galactosidase in HEK293T cells (or in HeLa cells), which prevented monitoring syncytium formation by X-Gal staining. However, there were no multinucleated structures in cocultures of HeLa-P4 cells with cells expressing the W596M mutant, and we found no evidence for mixing of their cytoplasm in another assay (see below).

To monitor membrane lipid exchanges, transfected HEK293T cells were labeled with DiO and left in contact for 2 h with DiI-labeled HeLa-P4 cells. In this experimental setting, expression of WT LAI Env resulted in ~8% double-fluorescent cells among the total number of cells analyzed (Fig. 5C). The background level was slightly higher than that in other experiments with HeLa-P4 target cells (~2%) but again was similar when HEK293T cells were mock transfected or transfected with an R5 Env expression vector (data not shown). Expression of the L568A Env mutant resulted in a low level of fluorescent dye exchange (~3%), relatively close to the background level (Fig. 5C), a finding which seems to be in agreement with the low efficiency of formation of syncytia
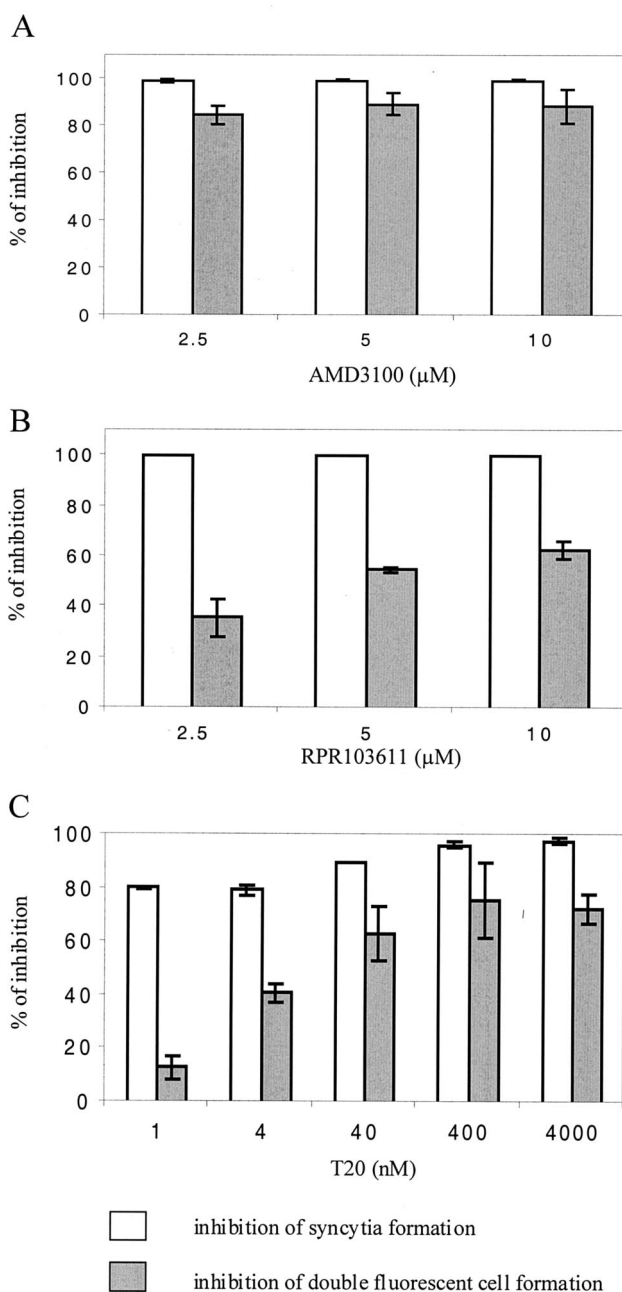

FIG. 3. Effect of inhibitors of HIV-1 entry on membrane exchanges and syncytium formation. Cocultures of DiI-labeled HeLa-P4 cells and DiO-labeled HeLa-Env/LAI cells were initiated at 4°C in the absence of inhibitor (2 h) and then shifted to 37°C in the presence or absence of the indicated concentration of AMD3100 bicyclam (A), betulinic acid derivative RPR103611 (B), or T20 peptide (C). Double-fluorescent cells were quantified by flow cytometry after 3 h at 37°C as described in the legend of Fig. 1, while syncytia were scored the next day in parallel cocultures by staining with X-Gal. The inhibition of membrane exchanges was calculated after subtracting the background level of double-fluorescent cells corresponding to coculture of labeled HeLa-P4 and Env-negative HeLa cells. Results are the mean values from two (T20) or three independent experiments.
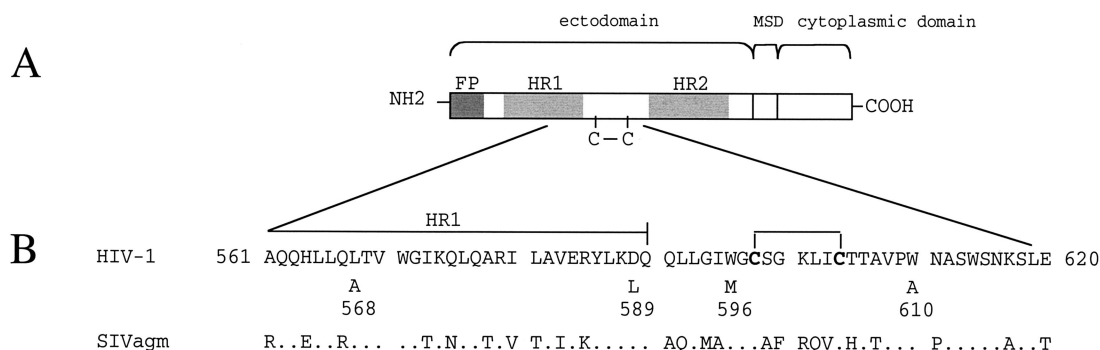
FIG. 4. Position of mutations in the HIV-1 gp41 ectodomain. (A) Schematic organization of retroviral transmembrane envelope glycoproteins. FP, fusion peptide; HR1 and HR2, N- and C-terminal helix regions; C—C, conserved Cys residues with disulfide link; MSD, membrane-spanning domain. (B) Partial sequence of the gp41 of HIV-1 LAI and of the homologous region from SIVagm. The positions of mutations are shown with the type of amino acid substituted. Numbering corresponds to the HIV-1 Env precursor (initial residue of gp41 at position 511).

mediated by this mutant (17% of WT Env). This result confirmed that gp41 has a direct role in the exchanges of fluorescent probes between Env$^+$ and target cells detected by the flow cytometry assay. In contrast, the other gp41 mutations tested seem to have little or no effect on these exchanges, since the fractions of double-fluorescent cells were similar when HEK293T cells expressed the WT LAI Env or the D589L mutant and were markedly higher than background when the W610A or the W596M Env mutant was expressed (Fig. 5C). This result suggested that these mutations blocked the cell-cell fusion process at a step occurring posterior to the merging of lipid bilayers.

We sought to obtain more direct evidence for this phenomenon by confocal microscopy. A significant fraction of the DiI or DiO labeling appears to be intracellular, either due to endocytosis of soluble probe or to the turnover of the plasma membrane. Intracellular labeling facilitates the detection of syncytia in cocultures of HeLa-P4 cells and cells stably expressing the WT Env (Fig. 6b). This type of image was not detected in cocultures with cells stably expressing the D589L or the W596M mutant Env, but there was evidence for efficient exchange of fluorescent probe between the plasma membranes of adjacent cells (Fig. 6c and d).

Detection of cytoplasmic exchanges. To address the possible effects of gp41 mutations on fusion pore formation, Env$^+$ and target cells were labeled with distinct fluorescent cytoplasmic probes, and double-fluorescent cells were detected by flow cytometry. The HeLa-P4 target cells were labeled by uptake of the red fluorescent probe CMTMR, while HEK293T cells were cotransfected to express WT or mutant HIV-1 Env and the GFP. After a 2-h coculture, double-fluorescent cells represented ~5.5% of analyzed cells when the WT Env was expressed and ~1.5% of cells in the absence of Env or when cells expressed the three mutant Env proteins (D589L, W596M, and W610A) previously found to mediate membrane exchanges but not syncytium formation (Fig. 7A). Since the size of GFP and the association of CMTMR with intracellular membranes could prevent their diffusion through small fusion pores, another series of experiments was performed with CMTMR-labeled HeLa-P4 cells and HEK293T cells labeled with the cytoplasmic fluorescent probe CTG (M_r, 465). In that case, formation of double-fluorescent cells was assayed by fluores-

cence microscopy and not by flow cytometry due to the lesser intensity of green fluorescence obtained with CTG. Double-fluorescent cells indicating cytoplasmic exchanges could be detected upon expression of the different gp41 mutants, but they were markedly less frequent than those found with WT gp41 (Fig. 7B). Numbers were relatively higher for the D589L and W596M mutants (~20% of WT) than for the L568A and W610A mutants (<10% of WT). The mutations in the loop region of gp41 therefore seem to affect the formation and dilation of fusion pores that are permeable to relatively small soluble molecules.

DISCUSSION

The flow cytometry assay used in this study was set up to address the initial steps of the cell-cell fusion process mediated by the HIV-1 gp41 TM, i.e., the merging of lipid bilayers corresponding to the plasma membranes of cells expressing HIV-1 Env and target cells. The completion of this step was deduced from the formation of double-fluorescent cells in cocultures of Env$^+$ and target cells labeled with distinct lipophilic green or red fluorescent probes (DiI or DiO). As for syncytia (or HIV-1 entry), the formation of double-fluorescent cells only occurred when Env$^+$ cells expressed a type of gp120 SU envelope protein (X4 or R5) matching the type of chemokine receptor (CXCR4 or CCR5) expressed on target cells. Only a background level of double fluorescence was detected in other situations or when cocultures of X4 Env$^+$ and target cells were performed in the presence of AMD3100, a CXCR4 antagonist. But cell-cell contacts mediated by SU-receptor interactions were not sufficient to allow transfer of fluorescent probe. A substitution in the N-terminal helix (HR1) of gp41 (L568A) was indeed found to markedly reduce the formation of both double-fluorescent cells and syncytia between Env$^+$ and target cells. Since the interaction of gp120 with CXCR4 should not be affected in this situation, it can be inferred that double-fluorescent cells result from membrane exchanges mediated by gp41.

The flow cytometry assay we have developed can therefore be considered a valid tool for functional studies of gp41 and can represent an alternative to microscopy-based techniques previously used to detect transfer of fluorescent dyes between
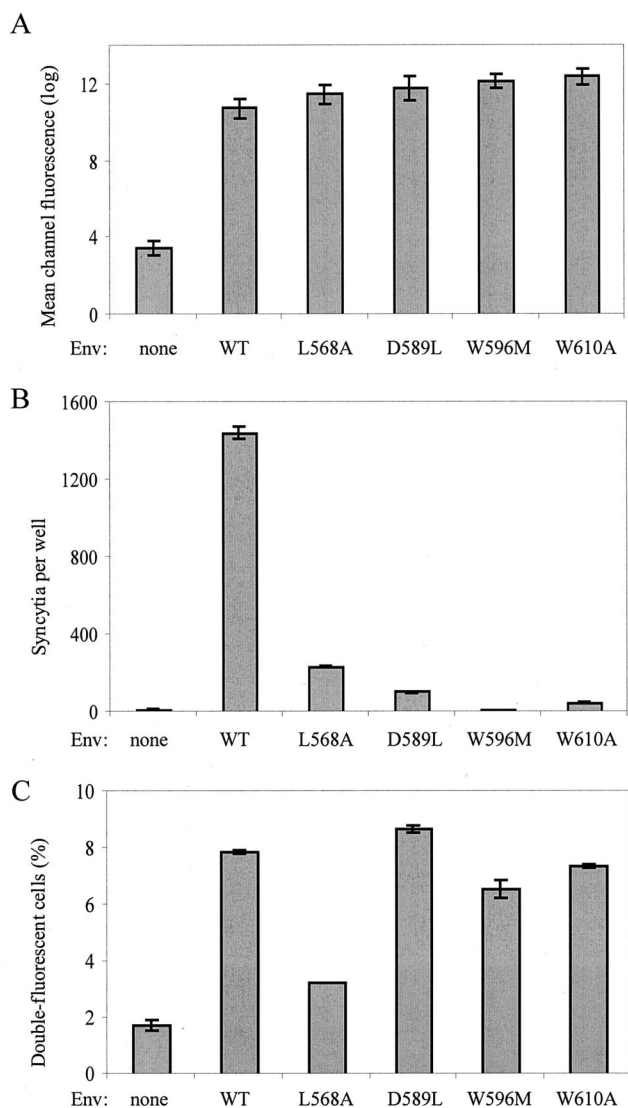
FIG. 5. Effect of mutations in gp41 on membrane exchanges and syncytium formation. (A) Expression of WT and mutant HIV-1 Env determined by flow cytometry after staining transfected HEK293T cells with a polyclonal anti-gp120 antibody and FITC-coupled secondary antibody. Bars represent mean channel fluorescence (arbitrary log units). (B) Formation of syncytia after overnight cocultures of ~2 × 10^5 HeLa-P4 cells and an equivalent number of transfected HEK293T cells. Syncytia were scored as blue foci after staining with X-Gal, or they were scored as multinucleated structures in the case of mutant W596M, due to the induction of a high β-galactosidase background upon transfection. (C) Formation of double-fluorescent cells after 2-h coculture of DiI-labeled HeLa-P4 cells and DiO-labeled transfected HEK293T cells. Coculture and flow cytometry analysis were performed as described in the legend of Fig. 1. All the gp41 mutants were tested in parallel. Results represent the means of three or four experiments ± standard errors of the means.
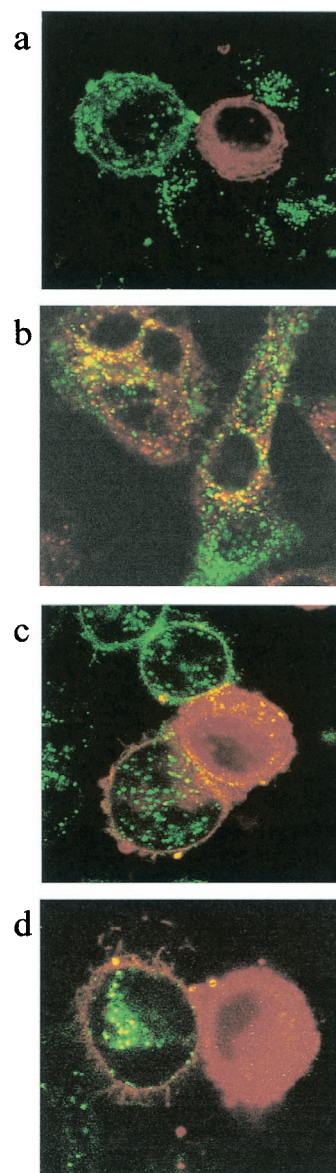

FIG. 6. Detection of membrane exchanges by confocal microscopy. Cocultures were initiated by adding DiI-labeled HeLa-P4 cells onto adherent DiO-labeled HeLa cells (glass coverslips) that were either Env negative (a) or stably expressing WT LAI Env (b) or the derived mutant Env D589L (c) or W596M (d). Cells were fixed after 2 h and analyzed on a Leica DMIRE2 microscope under ×63 magnification, ×2.5 zoom. Images were pseudocolored according to their respective emission wavelengths and overlaid by using Metamorph software.

membranes (38). The obvious advantage of assays based on flow cytometry is that quantitative results are directly obtained, while assays with a fluorescence microscopy readout require a statistical analysis of randomly selected fields. Our assay or the three-color flow cytometry assay recently described by Lin et al. (31) can also be performed with Env$^+$ cells obtained by transient transfection. They seem therefore to be particularly convenient for structure-function studies based on the comparison of series of mutant proteins.

Effect of mutations in the loop region of the gp41 ectodomain. The ectodomain of HIV-1 gp41 and of other retroviral TMs are characterized by the presence of two heptad repeats (HR1 and HR2, N and C termini, respectively), which associate in the context of TM trimers to form a tight proteinase-resistant six-helix bundle. It consists of an inner coiled coil formed by three parallel HR1s and three antiparallel HR2s
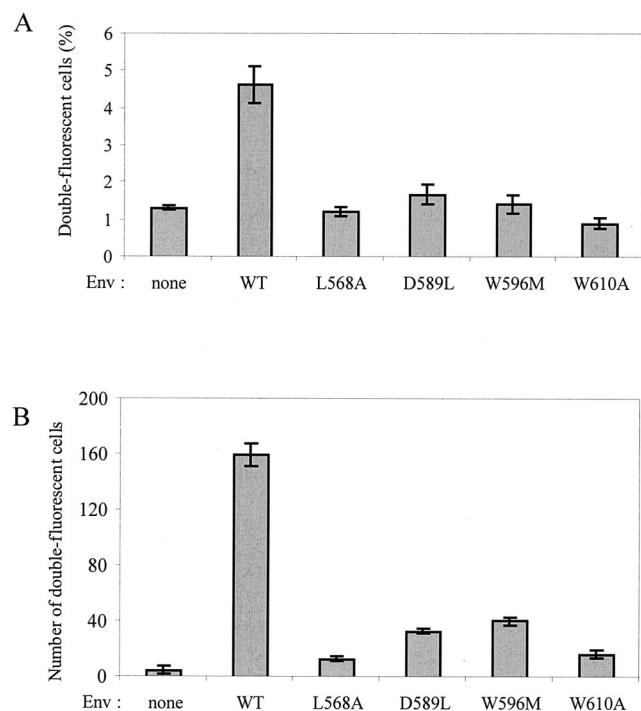
FIG. 7. Detection of cytoplasmic exchanges mediated by WT or mutant HIV-1 Env with different fluorescent probes. (A) HEK293T cells were transfected to express WT or mutant HIV-1 Env and the GFP and left in contact with HeLa-P4 cells labeled with the cytoplasmic dye CMTMR (red fluorescence). After a 2-h coculture, cells were detached, fixed, and analyzed by two-color flow cytometry. Bars represent percentages of cells with emission that was >3 log units in the red and green wavelengths (means of two experiments). The GFP and Env vectors were in a 1/4 ratio. A control plasmid was used instead of the Env vector to determine background. (B) Results of an experiment identical to that described in panel A, except that HEK293T cells were transfected only with Env vectors and then labeled by uptake of a low-molecular-weight green fluorescent probe, CTG. Cells were fixed in situ after coculture and observed under fluorescence microscopy. Bars represent the numbers of cells emitting fluorescence in both the green and red wavelengths counted in three random fields at ×40 magnification (results are the means ± standard errors of the means of two experiments).

green monkey retrovirus SIVagm, for which an ectodomain fragment including the loop region was analyzed by nuclear magnetic resonance (6). In this context, the Asp589, Trp596, and Trp610 residues are part of a hydrophobic cluster, corresponding to the last turn of the HR1 α-helix and the adjacent part of the loop region, proposed to represent a gp120 binding surface. If the HIV-1 gp41 adopts the same conformation, the mutations we have tested may therefore affect the stability of the SU/TM complex. Cao et al. (8) have indeed observed that the gp120 association index was reduced by the D589L and W596M mutations (44 and 60% of WT, respectively), while Maerz et al. found that substitutions at Trp596 and Trp610 reduced the fraction of cell-associated gp120 (33). But the lesser stability of the gp120/gp41 complex did not seem sufficient to account for the functional defects of these mutants. Indeed, other mutations reducing the gp120 association index in a similar way, e.g., F673P or E647L (42 and 43% of WT, respectively), had no apparent effect on syncytium formation (8). Moreover, mutations affecting the stability of the gp120/gp41 complex can be expected to inactivate gp41, like the shedding of gp120 induced by soluble CD4 (37) or by neutralizing anti-gp120 antibodies (42). On the contrary, we found that membrane exchanges between Env+ and target cells were not affected by the D589L mutation and were less affected than was syncytium formation by the W596M or W610A mutations. These results can therefore be viewed as an evidence that the gp41 ectodomain mediates events of the membrane fusion process that take place after the merging of membranes (hemifusion). Although indirect conformational effects cannot be ruled out, the fact that mutations of three distinct residues located on both sides of the cysteine motif had similar effects is in favor of a direct role of the loop region in these events. Several other mutations in this region of HIV-1 gp41 were recently found to prevent cell-cell fusion (33), and it will be of great interest to address their effects on the early steps of membrane fusion. The loop region of other retroviral TMs should also be examined for the possible conservation of this function.

The tryptophan-rich region of the HIV-1 ectodomain, located between the C-terminal helix (HR2) and the membrane-spanning domain, has been implicated in postmembrane exchange steps of the fusion process. Replacing five Trp residues in this region by Ala residues was indeed found to block syncytium formation and HIV-1 entry (45) but not exchanges of fluorescent membrane probes detected in a microscopy-based assay (39). The latter study found that the W(1-5)A mutant enabled exchanges of fluorescent cytoplasmic dyes such as calcine between Env+ and target cells, which suggests that fusion pores could form but not expand. In our study, the loop region mutants markedly reduced cytoplasmic exchanges assayed with CTG, a small fluorescent probe (10 to 20% of the level seen with WT gp41) and apparently blocked exchanges of a larger fluorescent molecule (GFP). The mutations in the loop region of gp41 therefore seem to affect both the formation of fusion pores and their expansion. Parallel assays are clearly required to confirm these functional differences between the loop region and membrane-proximal domain of gp41.

How the loop region of HIV-1 gp41 and other retroviral TMs may contribute to the formation of a fusion pore or to

packed in its external grooves (6, 9, 51). The loop region intervening between HR1 and HR2 allows the reversal of chain orientation required to form the so-called hairpin structure (6). It is also remarkable because of the presence of disulfide-linked cysteine residues forming a Cys-(X)$_{5-7}$-Cys motif and by the presence of an immunodominant B epitope in the case of HIV-1 and other lentiviruses (12, 22).

In this study, we addressed the effect of different mutations of the ectodomain of HIV-1 gp41 at residues located in the loop region on both sides of the disulfide-linked motif (W596 M and W610A) or in the distal part of the N-terminal helix (D589L). These mutations were selected because they markedly reduce the efficiency of syncytium formation but do not affect the overall expression of Env and did not seem to disrupt a known functional element of gp41, unlike mutations in the fusion peptide or at hydrophobic residues of the heptad repeats (e.g., L568A). The Asp589, Trp596, and Trp610 residues of HIV-1 gp41 are conserved in the gp41 of the related African

later events cannot be deduced from our observations. In the case of the influenza virus fusogenic protein (HA2), a relatively high local density seems to be an important parameter for the completion of later steps of the membrane fusion process (11). By analogy with this model, it may be envisioned that the gp41 loop region or the Trp-rich domain mediates interactions between different gp41 trimers, thereby allowing them to reach a critical local density. But mutations in the loop region may also have an indirect effect on the association of gp41 trimers by reducing the stability of the six-helix bundle. The loop region of SIV gp41 was indeed found to increase the stability of the trimeric helical hairpin, either in solution or in the presence of membranes (40).

Post-lipid mixing activity of antiviral agents. Two unrelated HIV-1 entry inhibitors were found to have a limited effect on lipid exchanges between Env$^+$ and target cells at concentrations that blocked or markedly reduced the formation of syncytia. One was T20 (or DP178), a 36-residue peptide corresponding to most of the C-terminal helix and adjacent membrane-proximal domain. Our results are in good agreement with previous observations, made in a different experimental setting, that the inhibitory activity of T20 is exerted, at least in part, after the merging of lipid bilayers (26, 38). More recently, Markosyan et al. proposed that C34, another antiviral peptide derived from the HR2 region of gp41, may be acting after the formation of labile fusion pores (35). Post-lipid mixing effects of T20 and related peptides may modify some of the present views on mechanisms of membrane fusion mediated by gp41 and other retroviral TMs, in particular the hypothesis of a prehairpin structure in which HR1 and HR2 are dissociated (51). This structure has not been directly observed but was considered necessary to account for the antiviral activity of HR2 peptides in that it allowed access to their putative target, the N-terminal helix of gp41, which is buried within the six-helix bundle structure (hairpin). Also, transition of gp41 from metastable prehairpin to stable hairpin structure was proposed to drive the merging of membranes (10, 51). But the hypothesis of a prehairpin structure may not be required if HR2 peptides can exert their antiviral activity after the membranes have merged, as was suggested by our results and those of others, and if their actual target is not HR1. Residues within HR1 were found to determine the sensitivity of HIV-1 to T20 and other HR2 peptides, but these results were obtained with laboratory strains selected in the presence of high concentrations of peptides (44). There are indications that other regions of gp41 can be involved in the susceptibility of HIV-1 to this class of antiviral agents (16). More thorough analysis of in vivo-selected resistant strains will help to clarify this issue.

The second compound was RPR103611, a low-molecular-weight (M_r, 755) derivative of betulinic acid blocking the cell entry of X4 HIV-1 strains and the formation of syncytia (36). We have proposed that its target was gp41, not gp120, based on the kinetics of the antiviral effect and on the identification of different mutations conferring drug resistance in the loop region of the ectodomain (29, 30). The finding that cell-cell fusion can be blocked with limited effects on membrane exchanges seems to confirm our hypothesis regarding the RPR103611 target and is consistent with the role of the loop region of the ectodomain in late steps of the fusion process. Indeed, complete drug resistance was conferred by substitu-

tions of an isoleucine at position 595 (I595S), therefore adjacent to Trp 596, or of a leucine at position 602 (L602H) within the disulfide-linked motif (29, 30). This result stresses the importance of hydrophobic residues, both in the loop and membrane-proximal regions, in the late steps of the fusion process.

REFERENCES

1. **Baker, K. A., R. E. Dutch, R. A. Lamb, and T. S. Jardetzky.** 1999. Structural basis for paramyxovirus-mediated membrane fusion. Mol. Cell **3:**309–319.
2. **Berger, E. A., P. M. Murphy, and J. M. Farber.** 1999. Chemokine receptors as HIV-1 coreceptors: roles in viral entry, tropism, and disease. Annu. Rev. Immunol. **17:**657–700.
3. **Blumenthal, R., M. J. Clague, S. R. Durell, and R. M. Epand.** 2003. Membrane fusion. Chem. Rev. **103:**53–69.
4. **Brelot, A., and M. Alizon.** 2001. HIV-1 entry and how to block it. AIDS **15:**S3–S11.
5. **Bullough, P. A., F. M. Hughson, J. J. Skehel, and D. C. Wiley.** 1994. Structure of influenza haemagglutinin at the pH of membrane fusion. Nature **371:**37–43.
6. **Caffrey, M., M. Cai, J. Kaufman, S. J. Stahl, P. T. Wingfield, D. G. Covell, A. M. Gronenborn, and G. M. Clore.** 1998. Three-dimensional solution structure of the 44 kDa ectodomain of SIV gp41. EMBO J. **17:**4572–4584.
7. **Caffrey, M., J. Kaufman, S. J. Stahl, P. T. Wingfield, A. M. Gronenborn, and G. M. Clore.** 1999. Monomer-trimer equilibrium of the ectodomain of SIV gp41: insight into the mechanism of peptide inhibition of HIV infection. Protein Sci. **8:**1904–1907.
8. **Cao, J., L. Bergeron, E. Helseth, M. Thali, H. Repke, and J. Sodroski.** 1993. Effects of amino acid changes in the extracellular domain of the human immunodeficiency virus type 1 gp41 envelope glycoprotein. J. Virol. **67:**2747–2755.
9. **Chan, D. C., D. Fass, J. M. Berger, and P. S. Kim.** 1997. Core structure of gp41 from the HIV envelope glycoprotein. Cell **89:**263–273.
10. **Chan, D. C., and P. S. Kim.** 1998. HIV entry and its inhibition. Cell **93:**681–684.
11. **Chernomordik, L., V. A. Frolov, E. Leikina, P. Bronk, and J. Zimmerberg.** 1998. The pathway of membrane fusion catalyzed by influenza hemagglutinin: restriction of lipids, hemifusion, and lipidic fusion pore formation. J. Cell Biol. **140:**1369–1382.
12. **Chong, Y.-H., J. M. Ball, C. J. Issel, R. C. Montelaro, and K. E. Rushlow.** 1991. Analysis of equine humoral responses to the transmembrane envelope glycoprotein (gp45) of equine infectious anemia virus. J. Virol. **65:**1013–1018.
13. **Clavel, F., and P. Charneau.** 1994. Fusion from without directed by human immunodeficiency virus particles. J. Virol. **68:**1179–1185.
14. **Colman, P. M., and M. C. Lawrence.** 2003. The structural biology of type 1 viral membrane fusion. Nat. Rev. Mol. Cell Biol. **4:**309–319.
15. **De Clercq, E., N. Yamamoto, R. Pauwels, M. Baba, D. Schols, H. Nakashima, J. Balzarini, Z. Debyser, B. A. Murrer, D. Schwartz, D. Thornton, G. Bridger, S. Fricker, G. Henson, M. Abrams, and D. Picker.** 1992. Potent and selective inhibition of human immunodeficiency virus (HIV)-1 and HIV-2 replication by a class of bicyclams interacting with a viral uncoating event. Proc. Natl. Acad. Sci. USA **89:**5286–5290.
16. **Derdeyn, C. A., J. M. Decker, J. N. Sfakianos, Z. Zhang, W. A. O'Brien, L. Ratner, G. M. Shaw, and E. Hunter.** 2001. Sensitivity of human immunodeficiency virus type 1 to fusion inhibitors targeted to the gp41 first heptad repeat involves distinct regions of gp41 and is consistently modulated by gp120 interactions with the coreceptor. J. Virol. **75:**8605–8614.
17. **Doms, R. W.** 2001. Chemokine receptors and HIV entry. AIDS **15**(Suppl. 1):S34–S35.
18. **Dubay, J. W., S. J. Roberts, B. H. Hahn, and E. Hunter.** 1992. Truncation of the human immunodeficiency virus type 1 transmembrane glycoprotein cytoplasmic domain blocks virus infectivity. J. Virol. **66:**6616–6625.
19. **Fass, D., S. C. Harrison, and P. S. Kim.** 1996. Retrovirus envelope domain at 1.7 Å resolution. Nat. Struct. Biol. **3:**465–469.
20. **Gabuzda, D. H., A. Lever, E. Terwilliger, and J. Sodroski.** 1992. Effects of deletions in the cytoplasmic domain on biological functions of human immunodeficiency virus type 1 envelope glycoproteins. J. Virol. **66:**3306–3315.
21. **Gallaher, W. R., J. M. Ball, R. F. Garry, M. C. Griffin, and R. C. Montelaro.** 1989. A general model for the transmembrane proteins of HIV and other retroviruses. AIDS Res. Hum. Retrovir. **5:**431–440.
22. **Gnann, J. W., Jr., J. A. Nelson, and M. B. A. Oldstone.** 1987. Fine mapping

of an immunodominant domain in the transmembrane glycoprotein of human immunodeficiency virus. J. Virol. **61:**2639–2641.

23. **Helseth, E., U. Olshevsky, C. Furman, and J. Sodroski.** 1991. Human immunodeficiency virus type 1 gp120 envelope glycoprotein regions important for association with the gp41 transmembrane glycoprotein. J. Virol. **65:**2119–2125.

24. **Jahn, R., T. Lang, and T. C. Südhof.** 2003. Membrane fusion. Cell **112:**519–533.

25. **Jiang, S., K. Lin, and M. Lu.** 1998. A conformation-specific monoclonal antibody reacting with fusion-active gp41 from the human immunodeficiency virus type 1 envelope glycoprotein. J. Virol. **72:**10213–10217.

26. **Kliger, Y., S. A. Gallo, S. G. Peisajovich, I. Muñoz-Barroso, S. Avkin, R. Blumenthal, and Y. Shai.** 2001. Mode of action of an antiviral peptide from HIV-1. Inhibition at a post-lipid mixing stage. J. Biol. Chem. **276:**1391–1397.

27. **Kobe, B., R. J. Center, B. E. Kemp, and P. Poumbourios.** 1999. Crystal structure of human T cell leukemia virus type 1 gp21 ectodomain crystallized as a maltose-binding protein chimera reveals structural evolution of retroviral transmembrane proteins. Proc. Natl. Acad. Sci. USA **96:**4319–4324.

28. **Labrosse, B., A. Brelot, N. Heveker, N. Sol, D. Schols, E. De Clercq, and M. Alizon.** 1998. Determinants for sensitivity of human immunodeficiency virus coreceptor CXCR4 to the bicyclam AMD3100. J. Virol. **72:**6381–6388.

29. **Labrosse, B., O. Pleskoff, N. Sol, C. Jones, Y. Hénin, and M. Alizon.** 1997. Resistance to a drug blocking human immunodeficiency virus type 1 entry (RPR103611) is conferred by mutations in gp41. J. Virol. **71:**8230–8236.

30. **Labrosse, B., C. Tréboute, and M. Alizon.** 2000. Sensitivity to nonpeptidic compound (RPR103611) blocking human immunodeficiency virus Env-mediated fusion depends on sequence and accessibility of the gp41 loop region. J. Virol. **74:**2142–2150.

31. **Lin, X., C. A. Derdeyn, R. Blumenthal, and E. Hunter.** 2003. Progressive truncations C terminal to the membrane-spanning domain of the simian immunodeficiency virus Env reduce fusogenicity and increase concentration dependence of Env for fusion. J. Virol. **77:**7067–7077.

32. **Lu, M., S. C. Blacklow, and P. S. Kim.** 1995. A trimeric structural domain of the HIV-1 transmembrane protein. Nat. Struct. Biol. **2:**1075–1082.

33. **Maerz, A. L., H. E. Drummer, K. A. Wilson, and P. Poumbourios.** 2001. Functional analysis of the disulfide-bonded loop/chain reversal region of human immunodeficiency virus type 1 gp41 reveals a critical role in gp120-gp41 association. J. Virol. **75:**6635–6644.

34. **Malashkevich, V. N., D. C. Chan, C. T. Chutkowski, and P. S. Kim.** 1998. Crystal structure of the simian immunodeficiency virus (SIV) gp41 core: conserved helical interactions underlie the broad inhibitory activity of gp41 peptides. Proc. Natl. Acad. Sci. USA **95:**9134–9139.

35. **Markosyan, R. M., F. S. Cohen, and G. B. Melikyan.** 2003. HIV-1 envelope proteins complete their folding into six-helix bundles immediately after fusion pore formation. Mol. Biol. Cell **14:**926–938.

36. **Mayaux, J.-F., A. Bousseau, R. Pauwels, T. Huet, Y. Hénin, N. Dereu, M. Evers, F. Soler, C. Poujade, E. De Clercq, and J.-B. Le Pecq.** 1994. Triterpene derivatives that block entry of human immunodeficiency virus type 1 into cells. Proc. Natl. Acad. Sci. USA **91:**3564–3568.

37. **Moore, J., J. McKeating, R. Weiss, and Q. Sattentau.** 1990. Dissociation of gp120 from HIV-1 virions induced by soluble CD4. Science **250:**1139–1142.

38. **Muñoz-Barroso, I., S. Durell, K. Sakaguchi, E. Appella, and R. Blumenthal.** 1998. Dilation of the human immunodeficiency virus-1 envelope glycoprotein fusion pore revealed by the inhibitory action of a synthetic peptide from gp41. J. Cell Biol. **140:**315–323.

39. **Muñoz-Barroso, I., K. Salzwedel, E. Hunter, and R. Blumenthal.** 1999. Role of the membrane-proximal domain in the initial stages of the human immunodeficiency virus type 1 envelope glycoprotein-mediated membrane fusion. J. Virol. **73:**6089–6092.

40. **Peisajovich, S. G., L. Blank, R. F. Epand, R. M. Epand, and Y. Shai.** 2003. On the interaction between gp41 and membranes: the immunodominant loop stabilizes gp41 helical hairpin conformation. J. Mol. Biol. **326:**1489–1501.

41. **Pleskoff, O., C. Treboute, A. Brelot, N. Heveker, M. Seman, and M. Alizon.** 1997. Identification of a chemokine receptor encoded by human cytomegalovirus as a cofactor for HIV-1 entry. Science **276:**1874–1878.

42. **Poignard, P., T. Fouts, D. Naniche, J. P. Moore, and Q. J. Sattentau.** 1996. Neutralizing antibodies to human immunodeficiency virus type-1 gp120 induce envelope glycoprotein subunit dissociation. J. Exp. Med. **183:**473–484.

43. **Poignard, P., E. O. Saphire, P. W. Parren, and D. R. Burton.** 2001. gp120: biologic aspects of structural features. Annu. Rev. Immunol. **19:**253–274.

44. **Rimsky, L. T., D. C. Shugars, and T. J. Matthews.** 1998. Determinants of human immunodeficiency virus type 1 resistance to gp41-derived inhibitory peptides. J. Virol. **72:**986–993.

45. **Salzwedel, K., J. T. West, and E. Hunter.** 1999. A conserved tryptophan-rich motif in the membrane-proximal region of the human immunodeficiency virus type 1 gp41 is important for Env-mediated fusion and virus infectivity. J. Virol. **73:**2469–2480.

46. **Schwartz, O., M. Alizon, J. M. Heard, and O. Danos.** 1994. Impairment of T cell receptor-dependent stimulation in CD4$^+$ lymphocytes after contact with membrane-bound HIV-1 envelope glycoprotein. Virology **198:**360–365.

47. **Skehel, J. J., and D. C. Wiley.** 2000. Receptor binding and membrane fusion in virus entry: the influenza hemagglutinin. Annu. Rev. Biochem. **69:**531–569.

48. **Stein, B. S., S. D. Gowda, J. D. Lifson, R. C. Penhallow, K. G. Bensch, and E. G. Engleman.** 1987. pH-independent HIV entry into CD4-positive T cells via envelope fusion to the plasma membrane. Cell **49:**659–668.

49. **Tan, K., J. H. Liu, J. H. Wang, S. Shens, and M. Lu.** 1997. Atomic structure of a thermostable subdomain of HIV-1 gp41. Proc. Natl. Acad. Sci. USA **94:**12303–12308.

50. **Weissenhorn, W., A. Carfi, K.-H. Lee, J. J. Skehel, and D. C. Wiley.** 1998. Crystal structure of the Ebola virus membrane fusion subunit, GP2, from the envelope glycoprotein ectodomain. Mol. Cell **2:**605–616.

51. **Weissenhorn, W., A. Dessen, S. C. Harrison, J. J. Skehel, and D. C. Wiley.** 1997. Atomic structure of the ectodomain from HIV-1 gp41. Nature **387:**426–430.

52. **Wild, C., T. Oas, C. McDanal, D. Bolognesi, and T. Matthews.** 1992. A synthetic peptide inhibitor of human immunodeficiency virus replication: correlation between solution structure and viral inhibition. Proc. Natl. Acad. Sci. USA **89:**10537–10541.

53. **Wilk, T., T. Pfeiffer, A. Bukovsky, G. Moldenhauer, and V. Bosch.** 1996. Glycoprotein incorporation and HIV-1 infectivity despite exchange of the gp160 membrane-spanning domain. Virology **218:**269–274.

54. **Wyatt, R., and J. Sodroski.** 1998. The HIV-1 envelope glycoproteins: fusogens, antigens, and immunogens. Science **280:**1884–1888.